EJN EUROPEAN JOURNAL OF NEUROSCIENCE

European Journal of Neuroscience, Vol. 38, pp. 2341–2348, 2013 doi:10.1111/ejn.12237

TECHNICAL SPOTLIGHT
Antibodies to cannabinoid type 1 receptor co-react with stomatin-like protein 2 in mouse brain mitochondria

Yury M. Morozov,[1] Martin H. Dominguez,[1] Luis Varela,[2] Marya Shanabrough,[2] Marco Koch,[2,3] Tamas L. Horvath[2] and Pasko Rakic[1]

[1]Department of Neurobiology, Yale University School of Medicine and Kavli Institute for Neuroscience, New Haven, CT, USA
[2]Program on Cell and Neurobiology of Energy Metabolism, Section of Comparative Medicine, Yale University School of Medicine, New Haven, CT, USA
[3]Institute of Anatomy, University of Leipzig, Leipzig, Germany

Keywords: antibody specificity, CB_1, marijuana, mitochondrial respiration, serology, SLP-2

Abstract

Anti-cannabinoid type 1 receptor (CB_1) polyclonal antibodies are widely used to detect the presence of CB_1 in a variety of brain cells and their organelles, including neuronal mitochondria. Surprisingly, we found that anti-CB_1 sera, in parallel with CB_1, also recognize the mitochondrial protein stomatin-like protein 2. In addition, we show that the previously reported effect of synthetic cannabinoid WIN 55,212-2 on mitochondrial complex III respiration is not detectable in purified mitochondrial preparations. Thus, our study indicates that a direct relationship between endocannabinoid signaling and mitochondrial functions in the cerebral cortex seems unlikely, and that caution should be taken interpreting findings obtained using anti-CB_1 antibodies.

Introduction

The application of antibodies for immunohistochemical identification of proteins guaranteed pronounced advances in cellular and molecular research of complex biological systems; for example, cannabinoid signaling in the mammalian brain (reviewed in DiPatrizio & Piomelli, 2012; Katona & Freund, 2012; Skaper & Di Marzo, 2012). Nevertheless, there are some technical issues that need to be taken into consideration. For example, determination of the molecular construct of the antigen's antibody-binding site (epitope; which might be composed of discontinuous sections of the antigen's amino acid sequence) is an extremely time-consuming procedure and is impractical to perform in full size for all currently applied sera (Mayrose *et al.*, 2007). As a result, serological identification of proteins might be uncertain and prone to misinterpretations.

Recently, we unexpectedly discovered that anti-cannabinoid type 1 receptor (CB_1) sera, in parallel with CB_1, also bind the mitochondrial protein stomatin-like protein 2 (SLP-2). Although we reported these results at the 2010 SFN annual meeting (Morozov *et al.*, 2010), these antibodies continue to be used to study the possible direct effect of endocannabinoids on mitochondrial energy utilization in neurons (e.g. Benard *et al.*, 2012). Here, we present the results of our investigation, which can help to clarify and re-interpret some of the conclusions based on the application of anti-CB_1 sera. Moreover, we also discovered that the reported effect of a synthetic cannabinoid on the respiratory activity of the isolated mitochondria (Benard *et al.*, 2012) depends critically upon the purity of mitochondrial fractions and may be replicated only in synaptosome-enriched, but not more pure, mitochondrial preparations.

Correspondences: Dr P. Rakic and Dr Y. Morozov, as above.
E–mails: pasko.rakic@yale.edu and yury.morozov@yale.edu

Received 7 February 2013, revised 26 March 2013, accepted 31 March 2013

Materials and methods

The experiments were carried out in accordance with the National Institutes of Health (USA) guidelines for animal care and use, and the experimental protocols were approved by the Institutional Animal Care and Use Committee of Yale University. For terminal surgery, the animals were deeply anesthetized with pentobarbital (0.03 mL/10 g of body weight).

Immunocytochemistry for light and electron microscopy

CD-1 mouse embryos and newborn mice of the following ages were used: embryonic day 12.5 (E12.5; $n = 4$ embryos from two litters); E13.5 ($n = 17$ embryos from five litters); E16.5 ($n = 10$ embryos from four litters); E17.5 ($n = 9$ embryos from three litters); and postnatal day 1 ($n = 3$). CB_1 knockout (KO) embryos and wild-type littermates (in CD-1 background; Ledent *et al.*, 1999) at E15.5 (for both, $n = 3$ embryos), and CB_1-KO embryos and heterogenic littermates at E13.5 (for both, $n = 4$ embryos), as well as adult CB_1-KO and wild-type littermates (for both, $n = 3$) generated in C57BL6 background and genotyped as previously described (generation was sponsored by NIMH, Bethesda, MD, USA; Zimmer *et al.*, 1999) were also analysed. The embryos were decapitated, and the embryo

brains were removed and immersed overnight in a fixative containing 4% paraformaldehyde, 0.2% picric acid and 0.2% glutaraldehyde. Postnatal mice were perfused transcardially by the same fixative prior to brain collection. Coronal brain sections were cut with a vibratome (100-μm-thick or 60-μm-thick sections for embryos or postnatal animals, respectively) and used for immunocytochemistry as described below.

About half of the embryo brain sections were immersed in 0.5% H_2O_2 for 30 min to block tissue peroxidase, whereas the remaining specimens were used for immunocytochemistry omitting this step. No difference in mitochondrial immunolabeling was detected in either case. The following polyclonal sera were used: anti-CB_1 against the last 31 amino acids (L31; C-terminus) of mouse CB_1 raised in guinea pig (Frontier Science, Japan; catalog no. CB1-GP-Af530-1; dilution 1 : 2000) or goat (Frontier Science, Japan; catalog no. CB1-Go-Af450; 1 : 1000); the last 15 amino acids (L15; C-terminus; 1 : 1000) or amino-terminus (NH; 1 : 4000) of rat CB_1 (both made in rabbit; gifts from K. Mackie, University of Washington, WA, USA). Biotinylated anti-guinea pig, anti-goat or anti-rabbit IgGs (1 : 300) and the Elite ABC kit (all from Vector Laboratories, Burlingame, CA, USA) with Ni-intensified 3,3′-diaminobenzidine-4HCl (DAB-Ni) as a chromogen were applied. Immunogold labeling of CB_1 was performed using goat anti-guinea pig IgG conjugated with 1-nm gold particles (1 : 80) and subsequent silver intensification with R-Gent SE-LM kit (all from Aurion, Wageningen, The Netherlands). Thereafter, sections were post-fixed with 0.5–1% OsO_4, dehydrated, and then embedded in durcupan (Fluka, Buchs, Switzerland) on microscope slides and coverslipped. Selected fragments of tissue were analysed and photographed with an Axioplan 2 microscope (Zeiss, Jena, Germany) and re-embedded into durcupan blocks for electron microscopic investigation. The samples were cut with a Reichert ultramicrotome into 70-nm-thick sections. The sections were then stained with lead citrate, and evaluated and photographed in a JEM 1010 electron microscope (JEOL, Japan) equipped with a Multiscan 792 digital camera (Gatan, Pleasanton, CA, USA). The specificity of the method and antibodies were confirmed by replacing primary antibodies with normal guinea pig serum (1 : 200; Jackson Immunoresearch, West Grove, PA, USA) or pre-absorption of both, made-in-guinea pig and made-in-goat, anti-CB_1 antisera with the antigene peptide (20 μg/mL; Frontier Science, Japan). Few, if any, mitochondrial staining was observed in these specimens either by light or electron microscopy.

Mitochondria/cytosol fractionation and Western blots analysis

Adult CD-1 mice ($n = 3$) or CD-1 mouse embryos at E16.5 ($n = 21$) were decapitated and brains were removed. Either single embryo brain or one adult cerebral hemisphere from adult mice were homogenized in an ice-cold tissue grinder with 0.5–1.0 mL cytosol extraction buffer mix containing dithiothreitol (DTT; 1 : 1000) and protease inhibitor cocktail (1 : 500; all from Calbiochem, La Jolla, CA, USA). The homogenates were centrifuged at 700 ***g*** for 10 min at +4 °C. Supernatants were transferred to fresh tubes and centrifuged at 10 000 ***g*** for 20 min at +4 °C. The second supernatants were collected as cytosolic fractions, whereas the pellets were resuspended in 100 μL of mitochondrial extraction buffer mix containing DTT (1 : 1000) and protease inhibitor cocktail (1 : 500; all from Calbiochem, La Jolla, CA, USA) and saved as mitochondrial fractions. The total protein content of all fractions was determined using the Bradford assay.

Based on protein content, 20-μg samples of the cytosolic and mitochondrial fractions were separated using electrophoresis in 4–12% NuPAGE Bis-Tris mini gels (Invitrogen, Carlsbad, CA, USA), and electrophoretically transferred to polyvinylidene fluoride membranes (Bio-Rad Laboratories, Hercules, CA, USA). The membranes were subsequently immunoblotted with anti-CB_1 (guinea pig; Frontier Science, Japan; 1 : 400), anti-SLP-2 (rabbit; 1 : 200; Santa Cruz Biotechnology, Santa Cruz, CA, USA) and anti-glyceraldehyde-3-phosphate dehydrogenase (mouse; 1 : 700; Chemicon International, Temecula, CA, USA) for load control. The membranes were counterstained using corresponding donkey anti-guinea pig (1 : 5000; Jackson Immunoresearch, West Grove, PA, USA), goat anti-rabbit or anti-mouse (both 1 : 3000; Bio-Rad Laboratories, Hercules, CA, USA) horseradish peroxidase conjugates. For stripping between the immunoblot procedures, membranes were rinsed and incubated in Restore Western Blot Stripping Buffer (Thermo Scientific, Rockford, IL, USA) according to the manufacturer's instructions. For visualization of the proteins, the membranes were exposed to the enhanced chemiluminescence detection system Lumigen PS-3 (1 : 40; GE Healthcare, Buckinghamshire, UK). No immunopositive bands were observed when immunoblotting was performed with anti-CB_1 antibodies pre-absorbed with the antigene peptide (5 μg/mL; Frontier Science, Japan).

Immunoprecipitation and mass spectrometry

For immunoprecipitation, ~2.0 mg of total protein from mouse embryo (E16.5) brain mitochondrial fractions (prepared as above) was incubated overnight at +4 °C with 3 μL of made-in-guinea pig anti-CB_1 sera (Frontier Science, Japan). Thirty microliters of a 1 : 1 slurry of protein A-sepharose (GE Healthcare, Buckinghamshire, UK) in phosphate-buffered saline was then added and antibody-bound protein was collected during a 2-h incubation at +4 °C. The Sepharose beads were washed four times in 500 μL phosphate-buffered saline containing protease inhibitor cocktail (1 : 500; Calbiochem, La Jolla, CA, USA). The beads and bound protein were loaded in mini gel and separated using electrophoresis as above. The gel was then stained with SimplyBlue colloidal Coomassie (Invitrogen, Carlsbad, CA, USA) following the manufacturer's instructions. The ~40-kDa band was cut from the gel and destained in three washes of acetic acid : methanol : H_2O (10 : 50 : 40) solution. The sample was submitted for in-gel tryptic digestion, followed by liquid chromatography, quadrupole/time-of-flight tandem mass spectrometry and peptide mass database searching (Keck Facility, Yale University, New Haven, CT, USA).

Cell culture and transfections

Mouse neuroblastoma 2A cells were cultured in Dulbecco's D-MEM/F12 medium containing 9% fetal bovine serum (all from Sigma-Aldrich, St Louis, MO, USA). For transfections, we cloned full-length SLP-2 from E14.5 embryo brain cDNA into pIRES2-EGFP (Clontech, Mountain View, CA, USA); transfections with pEGFP (Clontech, Mountain View, CA, USA) were used as negative controls. Newly passaged cells at about 70–80% confluency were starved of serum overnight and transfected with 5 μg SLP-2 DNA using Lipofectamine 2000 reagent (Invitrogen, Carlsbad, CA, USA) according to the manufacturer's guidelines. After 24 h, cells were washed in phosphate-buffered saline, and immediately scraped and lysed in RIPA buffer (Cell Signaling Technology, Danvers, MA, USA) containing protease (Roche, Indianapolis, IN, USA) and phosphatase (Sigma-Aldrich, St Louis, MO, USA) inhibitor cocktails. Insoluble material was pelleted at 8000 ***g*** for 10 min on a lab microcentrifuge, and the total protein content of the supernatant was

read using the Bradford assay. Western blot analysis of SLP-2 transfected cells as well as control transfected cells was performed as described above.

Mitochondrial respiration

Mouse brain homogenates were purified using a differential centrifugation method described earlier (Rosenthal *et al.*, 1987; Moreira *et al.*, 2003). For isolation of mitochondria-enriched fractions, adult female CD-1 mice ($n = 11$) were killed, and the cerebral cortex was immediately dissected and put on ice. Tissue was manually homogenized at +4 °C in 10 mL isolation buffer [in mM: mannitol, 225; sucrose, 75; HEPES, 5; EGTA, 1; bovine serum albumin (BSA), 1 mg/mL; protease type VIII, 0.3125 mg/mL from Sigma–Aldrich at pH 7.4] and centrifuged at 2000 ***g*** for 5 min. The pellet, including the synaptosomal layer, was resuspended in isolation buffer now containing 0.02% (w/v) digitonin and centrifuged at 12 000 ***g*** for 10 min. The pellet without the synaptosomal layer was resuspended in isolation buffer and centrifuged at 12 000 ***g*** for 10 min. The pellet was finally resuspended in 100 μL of resuspension buffer (in mM: mannitol, 225; sucrose, 75; HEPES, 5; at pH 7.4). For isolation of synaptosome-enriched fractions, adult female CD-1 mice ($n = 4$) were used, and the cerebral cortex was homogenized in 1.5 mL of isolation buffer [in mM: mannitol, 215; sucrose, 75; HEPES, 20; EGTA, 1; 0.1% (w/v) fatty acid-free BSA at pH 7.2] followed by centrifugation at 1300 ***g*** for 3 min. The supernatant was removed and the resuspended pellets were again centrifuged at 1300 ***g*** for 3 min. The two sets of supernatants were pooled, topped off with isolation buffer and centrifuged at 13 000 ***g*** for 10 min. The supernatant was discarded; the pellet was resuspended in isolation buffer and centrifuged at 10 000 ***g*** for 10 min. The pellet was resuspended in isolation buffer without EGTA and centrifuged at 10 000 ***g*** for 10 min. The final cell fragments containing pellet were resuspended in 50 μL of isolation buffer without EGTA.

For mitochondrial respiration analyses, 0.5 mg/mL protein was added into the reaction chamber of a Clark-type oxygen electrode (Hansatech Instruments, Norfolk, UK) set to +37 °C and filled with 1 mL respiration buffer (in mM: sucrose, 100; HEPES, 5; KCl, 100; KH_2PO_4, 2; EGTA, 10 μM; pH 7.4). Prior to application of oxidative substrates, WIN 55,212-2 (WIN; Biomol International LP, Plymouth, PA, USA; final concentration 0.05 μM), which was predissolved in dimethyl sulfoxide (DMSO; stock solution 100 mM; stored at −20 °C), or DMSO alone diluted in respiration buffer (1 : 2000) were added into the reaction chamber. Thirty seconds later, pyruvate (5 mM) and malate (2.5 mM) were added concomitantly as the oxidative substrates. To determine ADP-dependent respiration (complex III activity), ADP (2.5 mM) was added. For each sample obtained from one animal, the respiration values were analysed 2–3 times, averaged and calculated as a percentage of Control for each experimental group (Control, Vehicle or WIN). Data were analysed using the Graph-Pad Prism 5 program (GraphPad Software,

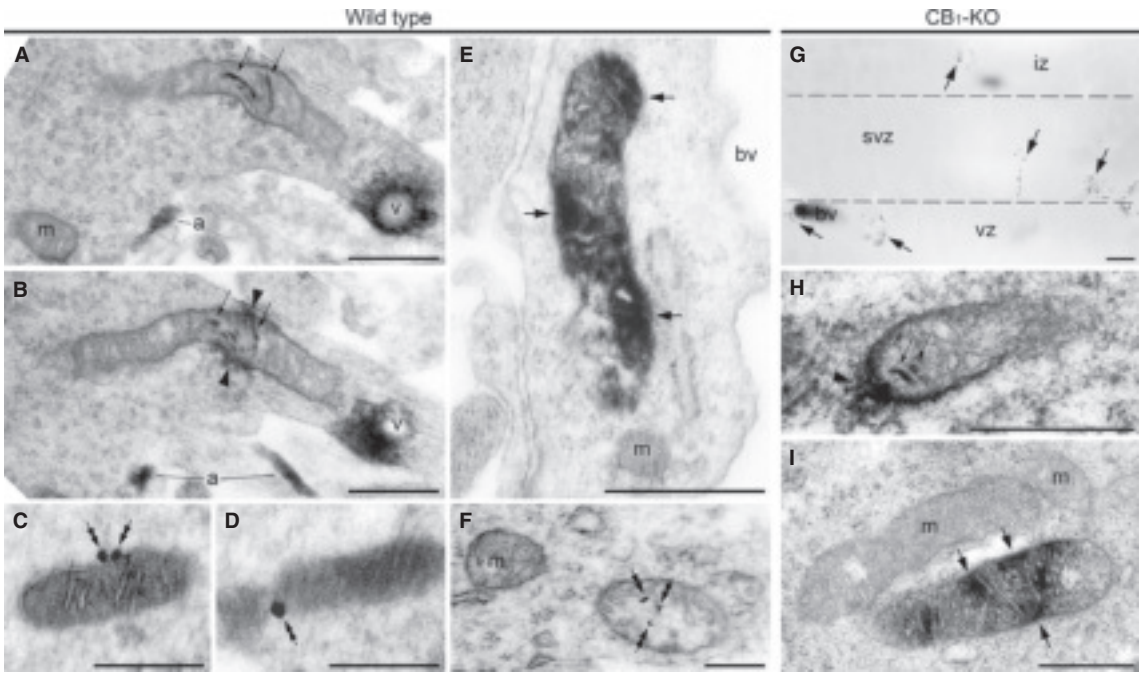

FIG. 1. Two types of anti-CB_1 immunolabeling of mitochondria in the immature brain of wild-type (A–F) and CB_1-KO (G–I) mice obtained using made-in-guinea pig anti-CB_1-L31 serum. (A and B) Serial micrographs of a type 1 mitochondrion in cerebral MZ at E13.5. Notice immunoprecipitation in the cristae (small arrows) and around the mitochondrion (arrowheads). Known patterns of anti-CB_1 immunolabeling are also seen (see, e.g. Morozov *et al.*, 2009), namely, in the neural processes – putative axons (a) and on the outer surface of intracellular vesicles (v). (C and D) Immunogold-silver particles (double arrows) on the outer surface of the mitochondrion seen in serial sections in the CA3 hippocampal zone of a newborn mouse. (E) A type 2 mitochondrion in an endothelial cell in the neocortex; notice robust staining in the mitochondrial matrix (arrows), whereas cristae remain immunonegative. (F) Immunogold-silver particles (double arrows) in the matrix of type 2 mitochondrion in the neocortical neuropil of a newborn mouse. (G–I) Anti-CB_1 immunolabeling in the CB_1-KO (C57BL6 background; Zimmer *et al.*, 1999) mouse embryo cerebrum at E13.5. (G) Light micrograph of the neocortex demonstrates numerous immunopositive particles (arrows) in the neuropil and blood vessels (bv), whereas CB_1-expressing axons and cell bodies are absent (see Morozov *et al.*, 2009). (H and I) Electron micrographs show that immunopositive particles seen in (G) represent mitochondria of both types identical to the labeling detected in wild-type animals. Notice stained cristae (small arrows) and staining outside the mitochondrion (arrowhead in H), or matrix staining (arrows in I). The borders between ventricular (vz), subventricular (svz) and intermediate (iz) zones of the embryonic cerebrum are demarked with dashed lines. Scale bars: 10 μm (G); 500 nm (A, B, E, H, I); 250 nm (C, D, F). m, immunonegative mitochondria.

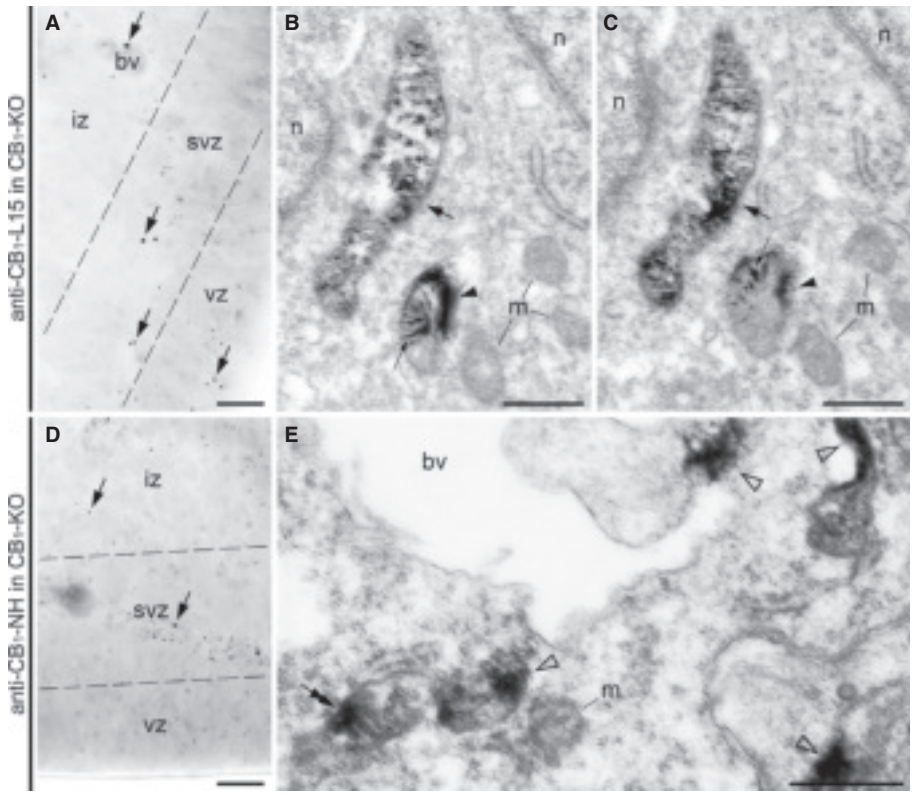

FIG. 2. Immunolabeling in the neocortex of CB_1-KO (CD-1 background; Ledent *et al.*, 1999) mouse embryos at E15.5 obtained using anti-CB_1-L15 (A–C) or anti-CB_1-NH (D and E) sera. (A and D) Light micrographs show that both sera produce similar immunopositive particles (arrows) in the neuropil and blood vessels, whereas CB_1-expressing axons and cell bodies are absent (see Morozov *et al.*, 2009). The borders between ventricular (vz), subventricular (svz) and intermediate zones (iz) of the embryonic cerebrum are demarked with dashed lines. (B and C) Serial electron micrographs show that most immunopositive particles labeled with anti-CB_1-L15 serum are either type 1 mitochondria, as indicated by stained cristae (small arrows) and labeling outside the mitochondria (arrowheads), or type 2 mitochondria as follows from immunoprecipitation in the matrix (arrows). (E) In contrast to the anti-CB_1-L15 serum, anti-CB_1-NH serum produced extensive background labeling (empty arrowheads) including occasional staining of mitochondria (double arrow). Scale bars: 10 μm (A, D); 500 nm (B, C, E). bv, lumen of blood vessel; m, immunonegative mitochondria; n, cell nucleus.

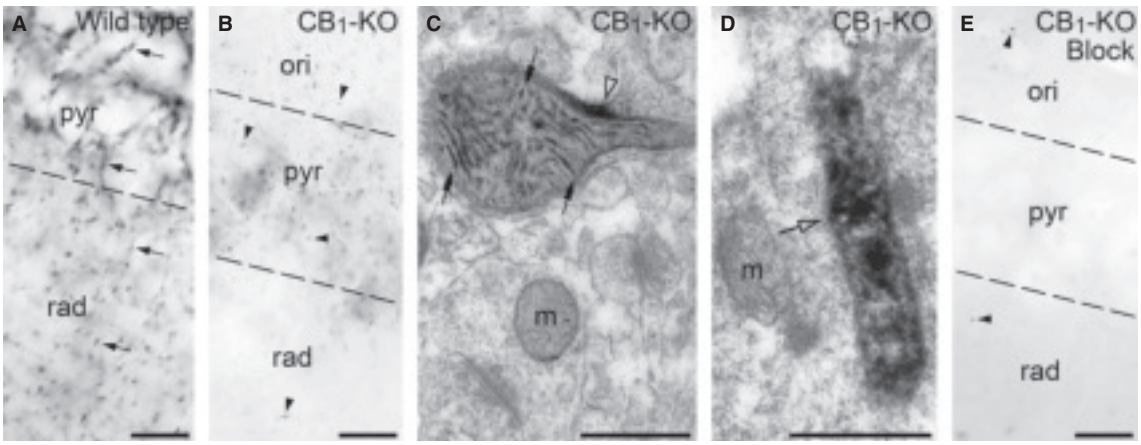

FIG. 3. Immunolabeling in the CA1 hippocampal zone of wild-type (A) and CB_1-KO (B–E; C57BL6 background; Zimmer *et al.*, 1999) adult mice using made-in-goat anti-CB_1-L31 serum (the same serum was used by Benard *et al.*, 2012). (A and B) Light microscopy displays typical CB_1-expressing axons (arrows) in the wild-type mouse (A); whereas only numerous stained particles are observed in sections of the CB_1-KO mouse (arrowheads in B), which by electron microscopy represent immunopositive mitochondria of both types 1 and 2. (C) A type 1 mitochondrion identified by DAB-Ni immunoprecipitation in the cristae (double arrows) and around the mitochondrion (empty arrowhead). (D) A type 2 mitochondrion identified by DAB-Ni immunoprecipitation in the matrix (empty arrow). (E) Mitochondrial imunolabeling is reduced by pre-absorption of the antibodies with the anti-gene peptide (L31 of CB_1), indicating that the antiserum selectively binds with the mitochondria. The borders between hippocampal layers are demarked with dashed lines. Scale bars: 10 μm (A, B, E); 500 nm (C, D). m, immunonegative mitochondria; ori, stratum oriens; pyr, stratum pyramidale; rad, stratum radiatum.

La Jolla, CA, USA) and expressed as the mean ± SEM. The means between two groups were analysed by unpaired *t*-test, and significant difference was taken at $P < 0.05$.

Following analyses of mitochondrial respiration, the remainder of each sample was processed for electron microscopy to confirm its mitochondrial or cell fragment content. This was accomplished by

centrifuging the remainder of each sample to obtain a pellet that was then immersion-fixed overnight in 4% paraformaldehyde, 0.2% picric acid and 0.1% glutaraldehyde. After post-fixation with 1% OsO_4, the samples were dehydrated and embedded in durcupan as above. Random fragments of the samples were cut into ultrathin sections, then stained with lead citrate as above and photographed in a JEM 1010 electron microscope (JEOL, Japan) at a magnification of 20 000×. The percentages of mitochondrial profiles in cell fragments among all the mitochondria were calculated in five random micrographs and then averaged.

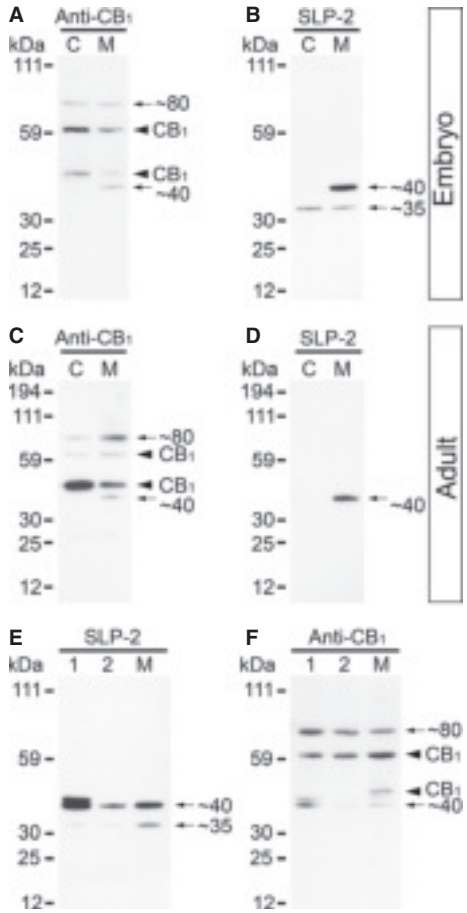

FIG. 4. Both anti-CB_1 (L31 made-in-guinea pig) and anti-SLP-2 sera recognize a ~40-kDa protein in Western blots. (A) In the mouse embryo brain preparations, besides glycosylated and deglycosylated forms of CB_1, which have molecular weights of 64 and 53 kDa, respectively (arrowheads), two other bands are detectable at approximately 40 and 80 kDa (arrows). Notice that the mitochondrial fraction (M) contains a ~40-kDa protein, which is absent from the cytosolic fraction (C). The mitochondrial fraction also contains CB_1, which can be due to contamination with CB_1-containing membrane fragments. (B) The membrane shown in (A) was stripped and reprobed with anti-SLP-2 antibodies revealing the ~40-kDa band (arrow) in the mitochondrial fraction (M) confirming our mass spectrometry identification of the protein. The anti-SLP-2 immunoblot also reveals a smaller form of SLP-2 seen here at approximately 35 kDa (arrow), which may represent a truncated form of SLP-2 (by data of the BLAST website computer analysis). (C and D) Anti-CB_1 (C) and anti-SLP-2 (D) Western blots of the same membrane show a similar set of proteins in adult mouse cerebrum. Note the inverted ratio of glycosylated and deglycosylated forms of CB_1 in the cytosolic fractions from embryonic and adult mice, and the absence of the 35-kDa SLP-2 in the adult mouse. (E and F) Anti-SLP-2 (E) and anti-CB_1 (F) Western blots of the same membrane. Columns '1' and '2' show proteins after transfection of SLP-2-IRES-EGFP and EGFP control, respectively, in N2A culture. Column 'M' shows the mitochondrial fraction from the mouse embryo brain. Transfection of SLP-2 noticeably increases the amount of the ~40-kDa protein (columns '1'), which is revealed as a doublet detectable with both anti-SLP-2 (E) and anti-CB_1 sera (F). Notice that only the heavy forms of SLP-2 are recognized by anti-CB_1 serum (A and F), suggesting that the truncated fragments of SLP-2 (see Fig. 5) are critical for binding of the anti-CB_1 antibodies.

Results

Binding of anti-CB_1 sera with mitochondria in the mouse brain

In our light and electron microscopic analyses of the distribution of CB_1 in the developing and adult mouse brain, we utilized: (i) a sensitive method of immunoperoxidase reaction with DAB-Ni as a chromogen; and (ii) a precise antigen location pre-embedding ultrasmall gold immunolabeling procedure with silver amplification. This enabled the detection of two hitherto unknown patterns of mitochondrial binding of anti-CB_1 (C-terminus) sera. One population of the immunopositive mitochondria, designated as 'type 1', contained DAB-Ni immunoreaction end-product on the outer membrane and in the cristae (Figs 1A, B and H, 2B and C, and 3C). This location of antigen on the outer surface of the mitochondrial membrane was confirmed by immunogold labeling (Fig. 1C and D), which very much resembles the immunolabeling recently demonstrated in the work of Benard *et al.* (2012). Although the staining of the cristae was less intense and below the limit of detection with the immunogold method, additional analysis (see below) suggested that it is, in fact, highly specific. The other type of immunopositive mitochondria, designated 'type 2', contained the antigen within the matrix; a finding also confirmed by immunogold labeling (Figs 1E, F and I, 2B and C, and 3D). The sera to different fragments of the C-terminus of CB_1, for example L15 and L31 (but not the NH-terminus), produced similar mitochondrial immunolabeling (Fig. 2), but most of our experiments were performed using anti-CB_1-L31 sera (see below). Patterns of mitochondrial immunolabeling with anti-CB_1-L31 sera were encountered both in embryos (Fig. 1) and in adult mice (Fig. 3). The specificity of these immunolabeling patterns is supported by our data showing that pre-absorption of the anti-CB_1 sera with the peptide (L31) abrogated the binding (Fig. 3E). Nevertheless, anti-CB_1 serum revealed a non-CB_1 peptide in the mitochondria as confirmed by equivalent immunolabeling patterns in wild-type and CB_1-KO mouse embryonic brain (generated in both CD-1 and C57BL6 genetic backgrounds), as well as adult brain (Figs 1–3).

The function of both types of immunopositive mitochondria in brain cells is unknown. The ratios of immunopositive mitochondria relative to immunonegative ones were generally small (less than 1%) in all specimens analysed, but they are relatively more frequent in sporadically distributed spots of neuropil and blood capillary cells in the embryo brain. In most cells, immunopositive mitochondria are situated adjacent to immunonegative ones. The density of immunopositive mitochondria in the adult animal is difficult to estimate accurately due to masking of the mitochondria by CB_1-containing axons at the resolution of light microscopy.

Antibodies to CB_1 recognize both CB_1 and SLP-2

To more definitively identify the mitochondrial target of anti-CB_1 sera, we performed immunoblot analysis of crudely fractionated mitochondria and cytosol from adult and embryonic mouse brain lysates. Among the four proteins immunopositive for anti-CB_1 sera, 64- and 53-kDa bands were seen in all specimens analysed (Fig. 4A) and likely represented CB_1 in glycosylated and deglycosylated forms, respectively (Song & Howlett, 1995; Fukudome *et al.*,

```
1   MLARRARGTG ALLLRGSVQA SGRVPRRASS GLPRNTVILF VPQQEAWVVE
51  RMGRFHRILE PGLNVLIPVL DRIRYVQSLK EIVINVPEQS AVTLDNVTLQ
101 IDGVLYLRIM DPYKASYGVE DPEYAVTQLA QTTMRSELGK LSLDKVFRER
151 EFLNANIVDA INQAADCWGI RCLRYEIKDI HVPPRVKESM QMQVEAERRK
201 RATVLESEGT RESAINVAEG KKQAQILASE AEKAEQINQA AGEASAVLAK
251 AKAKAEAIRI LAGALTQHNG DAAASLTVAE QYVSAFSKLA KDSNTVLLPS
301 NPSDVTSMVA QAMGVYGALT KAPVPGAQNS SQSRRDVQAT DTSIEELGRV
351 KLS
```

FIG. 5. Amino acid sequence of SLP-2 from data of the BLAST website (http://www.ncbi.nlm.nih.gov/blast/Blast.cgi). The amino acid sequences identified in our mass spectrometry assay are shown in red font. Underlined fragments are truncated from the 35-kDa form of SLP-2 that abrogates binding of anti-CB_1 antibodies in the Western blots.

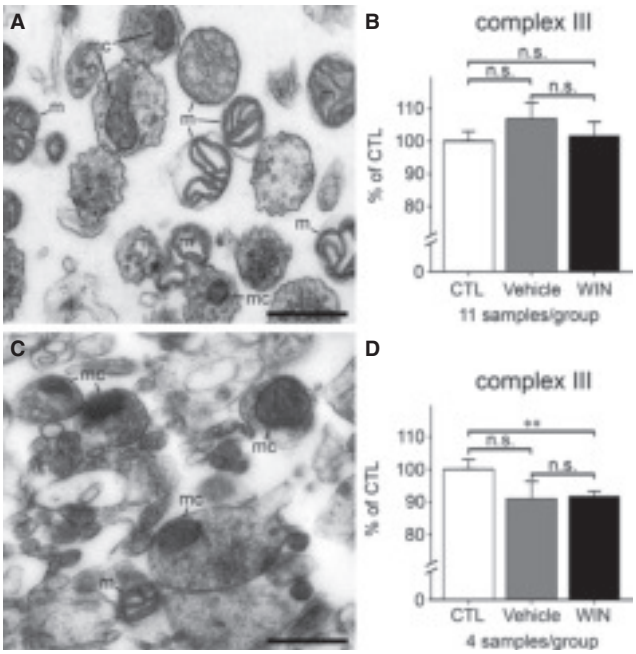

FIG. 6. Influence of the synthetic cannabinoid WIN on oxygen consumption in the mouse cerebral cortex homogenates of distinct content. (A) Representative electron micrograph of a pellet with predominating free mitochondria (m); the mitochondria inside cell fragments (mc) are also detectable. (B) In such mitochondrial fractions, WIN (50 nM) does not influence complex III respiration [CTL, 100% (172.6 ± 10.18 nmol/min/mg protein); Vehicle, 106.9%, n.s.; WIN, 101.5%, n.s.]. (C) Representative electron micrograph of a pellet showing numerous mc; m are also detectable. (D) In cell fragment-enriched preparations, WIN (50 nM) reduces complex III activity as compared with control, but not compared with the vehicle-treated preparations [CTL, 100% (95.24 ± 7.20 nmol/min/mg protein); Vehicle, 90.93%, n.s.; WIN, 91.64%; $^{**}P < 0.01$]. Scale bars: 500 nm.

2004). A low molecular weight band (~40 kDa) was detected only in the mitochondrial fractions from embryonic ($n = 21$; Fig. 4A) and adult brain ($n = 3$; Fig. 4C), and thus was a logical candidate for the target protein. We did not pursue the fourth band, an ~80-kDa protein, which was lightly immunolabeled in all mitochondrial ($n = 21$) and most cytosolic fractions analysed (14 of 21).

To further investigate the ~40-kDa protein, we isolated it from immunoprecipitates of the mitochondrial fraction of mouse embryo brain by simultaneous Coomassie Blue and immunoblot acrylamide gel electrophoresis; the protein was then subjected to mass spectrometric protein identification. Most notable among the results was that the sequenced peptides provided a > 50% homology with the known sequence of SLP-2 (Taylor *et al.*, 2003; Fig. 5). Basic local alignment search tool (BLAST) website computer analysis revealed the absence of homology between SLP-2 and the C-terminus of CB_1. Nevertheless, Western blots using anti-CB_1 and anti-SLP-2 sera demonstrated that the ~40-kDa band is equally detectable with either antibodies in the mitochondrial fractions of embryonic ($n = 19$; Fig. 4B) and adult brain ($n = 3$; Fig. 4C and D). Finally, to confirm the identification, we cloned SLP-2 from mouse embryo brain cDNA, and transiently transfected it in a mouse neuroblastoma (N2a) cell line. Transfection of SLP-2, but not control DNA, resulted in an increase in the ~40-kDa band to which both anti-SLP-2 and anti-CB_1 sera strongly reacted (Fig. 4E and F). Taken together, these results show that anti-CB_1 antibodies, in addition to recognizing CB_1, also recognize SLP-2, a mitochondrial inner membrane protein that faces the intermembrane space (Da Cruz *et al.*, 2008). Indeed, this finding corresponds well with our electron microscopic observations of type 1 mitochondria (Figs 1–3).

A direct effect of synthetic cannabinoid WIN on respiration of isolated mitochondria remains uncertain

To check the conclusion made by Benard *et al.* (2012) that cannabinoids may act directly upon mitochondrial CB_1, we replicated some of their experiments with isolated mouse brain mitochondria. From a methodology perspective of research on brain mitochondria, it is noteworthy to emphasize that isolation of purified mitochondria from the CNS is extremely difficult (Andrews *et al.*, 2008; Sims & Anderson, 2008; Wieckowski *et al.*, 2009). Despite following strict protocols of differential centrifugation equally applied in our and a published article (Benard *et al.*, 2012), we achieved unpredictable outcomes on mitochondrial purity; instead, the fractions always contained different amounts of synaptosomes (cell fragments containing cytoplasm and mitochondria entrapped within the intact cell membrane). That is why we performed mitochondrial respiration analysis in the fractions purified using two different protocols: the first, designed for concentrating free mitochondria; and the second, designed for production of synaptosomes (see Materials and methods). *Post hoc* electron microscopic examination revealed that the pellets prepared using these two protocols contain, on average, 25% (min 9%; max 52%) and 67% (min 54%; max 78%) of the

mitochondria situated in the cell fragments, respectively (Fig. 6A and C). In our experiments, the suppressive effect of WIN on complex III respiration (or mitochondrial respiration in terms of Benard *et al.*, 2012) could not be repeated in more pure mitochondrial fractions (Fig. 6B), but a similar effect was detected when the fractions contained increased amount of synaptosomes (Fig. 6D), which are known to contain CB_1 in the presynaptic cell membrane. It should be noted that our assay does not unequivocally demonstrate the effect of WIN on mitochondria transmitted through CB_1 situated in the cell membrane, because the differences between WIN-treated and vehicle-treated groups were not statistically significant.

Discussion

Our results show that anti-CB_1 immunolabeling in mitochondria is not specific for CB_1 as previously assumed in a recent publication (Benard *et al.*, 2012). The discrepancy between our findings and those of Benard *et al.* may be due to the fact that their results were based solely upon the application of a less sensitive ultra-small gold immunolabeling method with silver amplification. In the present study, we used the more sensitive immunoperoxidase reaction procedure with DAB-Ni as a chromogen. Moreover, we applied a combination of immunolabeling with both light (large field of observation) and electron microscopy (high resolution), which we consider crucial for confirmation of staining obtained by any single method. This approach allowed us to detect mitochondrial immunolabeling in CB_1-KO mice, which was likely missed by Benard and colleagues. The use of two anti-CB_1-L31 sera made in different hosts in our immunocytochemical, immunoprecipitation and Western blots studies also enabled identification of the mitochondrial protein SLP-2 that binds to anti-CB_1 antibodies. Anti-CB_1-L15 serum, which partially shares the amino acid sequence of the fusion peptide and might share the epitope of anti-CB_1-L31 sera, produces similar mitochondrial immunolabeling. Nevertheless, identification of SLP-2 with anti-CB_1-L15 serum should be taken with caution because we have not investigated or proved that it has the same specificity as anti-CB_1-L31 in the current investigation. The dual selectivity of anti-CB_1 sera has several hypothetical explanations. For example: (i) polyclonal anti-CB_1 sera might be contaminated with unidentified immunoglobulins; (ii) an unidentified sequence fragment may represent the SLP-2 epitope for anti-CB_1 antibodies; and/or (iii) binding of anti-CB_1 antibodies with the tertiary structure of SLP-2 (Mayrose *et al.*, 2007) may still retain some level of native confirmation under Western blot conditions. Understanding the basis of the dual selectivity of anti-CB_1 sera described here is an important topic for future research.

Because only one unique CB_1-immunopositive band was visible in our Western blot analysis of mitochondrial fractions, we hypothesize that SLP-2 is present in both type 1 and type 2 mitochondria designated here. However, in the case of type 2 mitochondria, SLP-2 is likely being misplaced due to disturbance in the intra-mitochondrial protein transport, whereby mitochondrial proteins synthesized in the cytoplasm are transported first to the mitochondrial matrix and later incorporated into the inner mitochondrial membrane (e.g. Stuart, 2002). Although SLP-2 is well expressed in the adult and developing mouse brain by high-resolution transcriptome analysis (see http://rakiclab.med.yale.edu/transcriptome.php; gene symbol Stoml2; Entrez gene ID 66592; Ayoub *et al.*, 2011) and is likely present in all mitochondria, we have detected it by immunolabeling in only a small number of mitochondria. We hypothesize that the previously demonstrated interaction of SLP-2 with phospholipids and prohibitins (Da Cruz *et al.*, 2008; Christie *et al.*, 2011), or its hetero-oligomer complexes with mitofusin 2 (Hajek *et al.*, 2007), block this protein from binding with anti-CB_1 antibodies in functional mitochondria. However, it appears that restructuring of proteins in some normal and pathological conditions results in the release of SLP-2 in both type 1 and type 2 mitochondria, which then become available for interaction with anti-CB_1 antibodies. Although we do not know the epitope of binding of anti-CB_1 antibodies, our unexpected finding opens the possibility of using anti-CB_1 sera as a novel tool for immunocytochemical exploration of the role of SLP-2 in mitochondria under normal and pathological conditions.

In summary, our ultrastructural and biochemical findings, together with analyses of mitochondrial oxygen consumption in association with cannabinoid signaling, indicate that a direct relationship between CB_1 and mitochondrial functions in the cerebral cortex is highly unlikely. We do not deny the validity of most studies that use CB_1 antibodies; however, we emphasize the need for additional controls and careful interpretation of immunolabeling results.

Acknowledgements

The authors are grateful to Ruth Rappaport, PhD, for her editorial assistance in the preparation of the manuscript. This research was supported by US Public Health Service. There were no conflicts of interest.

Abbreviations

BLAST, basic local alignment search tool; BSA, bovine serum albumin; CB_1, cannabinoid type 1 receptor; DAB-Ni, Ni-intensified 3,3′-diaminobenzidine-4HCl; DMSO, dimethylsulfoxide; DTT, dithiothreitol; E, embryonic day; KO, knockout; L15, last 15 amino acids; L31, last 31 amino acids; NH, amino-terminus; SLP-2, stomatin-like protein 2; WIN, WIN 55,212-2.

References

Andrews, Z.B., Liu, Z.W., Walllingford, N., Erion, D.M., Borok, E., Friedman, J.M., Tschöp, M.H., Shanabrough, M., Cline, G., Shulman, G.I., Coppola, A., Gao, X.B., Horvath, T.L. & Diano, S. (2008) UCP2 mediates ghrelin's action on NPY/AgRP neurons by lowering free radicals. *Nature*, **454**, 846–851.

Ayoub, A.E., Oh, S., Xie, Y., Leng, J., Cotney, J., Dominguez, M.H., Noonan, J.P. & Rakic, P. (2011) Transcriptional programs in transient embryonic zones of the cerebral cortex defined by high-resolution mRNA sequencing. *Proc. Natl. Acad. Sci. USA*, **108**, 14950–14955.

Benard, G., Massa, F., Puente, N., Lourenço, J., Bellocchio, L., Soria-Gómez, E., Matias, I., Delamarre, A., Metna-Laurent, M., Cannich, A., Hebert-Chatelain, E., Mulle, C., Ortega-Gutiérrez, S., Martőn-Fontecha, M., Klugmann, M., Guggenhuber, S., Lutz, B., Gertsch, J., Chaouloff, F., López-Rodrőguez, M.L., Grandes, P., Rossignol, R. & Marsicano, G. (2012) Mitochondrial CB_1 receptors regulate neuronal energy metabolism. *Nat. Neurosci.*, **15**, 558–564.

Christie, D.A., Lemke, C.D., Elias, I.M., Chau, L.A., Kirchhof, M.G., Li, B., Ball, E.H., Dunn, S.D., Hatch, G.M. & Madrenas, J. (2011) Stomatin-like protein 2 binds cardiolipin and regulates mitochondrial biogenesis and function. *Mol. Cell. Biol.*, **31**, 3845–3856.

Da Cruz, S., Parone, P.A., Gonzalo, P., Bienvenut, W.V., Tondera, D., Jourdain, A., Quadroni, M. & Martinou, J.C. (2008) SLP-2 interacts with prohibitins in the mitochondrial inner membrane and contributes to their stability. *Biochim. Biophys. Acta*, **1783**, 904–911.

DiPatrizio, N.V. & Piomelli, D. (2012) The thrifty lipids: endocannabinoids and the neural control of energy conservation. *Trends Neurosci.*, **35**, 403–411.

Fukudome, Y., Ohno-Shosaku, T., Matsui, M., Omori, Y., Fukaya, M., Tsubokawa, H., Taketo, M.M., Watanabe, M., Manabe, T. & Kano, M. (2004) Two distinct classes of muscarinic action on hippocampal inhibitory synapses: M2-mediated direct suppression and M1/M3-mediated indirect suppression through endocannabinoid signalling. *Eur. J. Neurosci.*, **19**, 2682–2692.

Hajek, P., Chomyn, A. & Attardi, G. (2007) Identification of a novel mitochondrial complex containing Mitofusin 2 and Stomatin-like protein 2. *J. Biol. Chem.*, **8**, 5670–5681.

Katona, I. & Freund, T.F. (2012) Multiple functions of endocannabinoid signaling in the brain. *Annu. Rev. Neurosci.*, **35**, 529–558.

Ledent, C., Valverde, O., Cossu, G., Petitet, F., Aubert, J.F., Beslot, F., Böhme, G.A., Imperato, A., Pedrazzini, T., Roques, B.P., Vassart, G., Fratta, W. & Parmentier, M. (1999) Unresponsiveness to cannabinoids and reduced addictive effects of opiates in CB1 receptor knockout mice. *Science*, **283**, 401–404.

Mayrose, I., Penn, O., Erez, E., Rubinstein, N.D., Shlomi, T., Freund, N.T., Bublil, E.M., Ruppin, E., Sharan, R., Gershoni, J.M., Martz, E. & Pupko, T. (2007) Pepitope: epitope mapping from affinity-selected peptides. *Bioinformatics*, **23**, 3244–3246.

Moreira, P.I., Santos, M.S., Moreno, A.M., Seiça, R. & Oliveira, C.R. (2003) Increased vulnerability of brain mitochondria in diabetic (Goto-Kakizaki) rats with aging and amyloid-beta exposure. *Diabetes*, **52**, 1449–1456.

Morozov, Y.M., Torii, M. & Rakic, P. (2009) Origin, early commitment, migratory routes, and destination of cannabinoid Type 1 receptor-containing interneurons. *Cereb. Cortex*, **19**, i78–i89.

Morozov, Y.M., Dominguez, M.H. & Rakic, P. (2010) *Mitochondrial Disorganization as an Early Detectable Sign of Neuronal and Endothelial Cells Distress During Development of Mouse Brain*. Program #871.11 Neuroscience Meeting Planner. Society for Neuroscience, San Diego, CA, 2010. Online.

Rosenthal, R.E., Hamud, F., Fiskum, G., Varghese, P.J. & Sharpe, S. (1987) Cerebral ischemia and reperfusion: prevention of brain mitochondrial injury by lidoflazine. *J. Cerebr. Blood F. Met.*, **7**, 752–758.

Sims, N.R. & Anderson, M.F. (2008) Isolation of mitochondria from rat brain using Percoll density gradient centrifugation. *Nat. Protoc.*, **3**, 1228–1239.

Skaper, S.D. & Di Marzo, V. (2012) Endocannabinoids in nervous system health and disease: the big picture in a nutshell. *Philos. T. Roy. Soc. B.*, **367**, 3193–3200.

Song, C. & Howlett, A.C. (1995) Rat cannabinoid receptors are N-linked glycosylated proteins. *Life Sci.*, **56**, 1983–1989.

Stuart, R. (2002) Insertion of proteins into the inner membrane of mitochondria: the role of the Oxa1 complex. *Biochim. Biophys. Acta*, **1592**, 79–87.

Taylor, S.W., Fahy, E., Zhang, B., Glenn, G.M., Warnock, D.E., Wiley, S., Murphy, A.N., Gaucher, S.P., Capaldi, R.A., Gibson, B.W. & Ghosh, S.S. (2003) Characterization of the human heart mitochondrial proteome. *Nat. Biotechnol.*, **21**, 281–286.

Wieckowski, M.R., Giorgi, C., Lebiedzinska, M., Duszynski, J. & Pinton, P. (2009) Isolation of mitochondria-associated membranes and mitochondria from animal tissues and cells. *Nat. Protoc.*, **4**, 1582–1590.

Zimmer, A., Zimmer, A.M., Hohmann, A.G., Herkenham, M. & Bonner, T.I. (1999) Increased mortality, hypoactivity, and hypoalgesia in cannabinoid CB_1 receptor knockout mice. *Proc. Natl. Acad. Sci. USA*, **96**, 5780–5785.